World Academy of Science, Engineering and Technology
International Journal of Electronics and Communication Engineering
Vol:7, No:6, 2013

# Exploiting Non Circularity for Angle Estimation in Bistatic MIMO Radar Systems

Ebregbe David, Deng Weibo



***Abstract*****—**The traditional second order statistics approach of using only the hermitian covariance for non circular signals, does not take advantage of the information contained in the complementary covariance of these signals. Radar systems often use non circular signals such as Binary Phase Shift Keying (BPSK) signals. Their noncicular property can be exploited together with the dual centrosymmetry of the bistatic MIMO radar system to improve angle estimation performance. We construct an augmented matrix from the received data vectors using both the positive definite hermitian covariance matrix and the complementary covariance matrix. The Unitary ESPRIT technique is then applied to the signal subspace of the augmented covariance matrix for automatically paired Direction-of-arrival (DOA) and Direction-of-Departure (DOD) angle estimates. The number of targets that can be detected is twice that obtainable with the conventional ESPRIT approach. Simulation results show the effectiveness of this method in terms of increase in resolution and the number of targets that can be detected.

***Keywords*****—**Bistatic MIMO Radar, Unitary Esprit, Non circular signals.

## I. Introduction

THE desire to correctly identify and obtain accurate estimates of target locations has prompted an increase in the study of Multiple Input Multiple Output (MIMO) radar systems. This follows from successes reported in MIMO Communications. Spatial diversity gain and waveform diversity are two very important advantages obtainable from MIMO radar systems [1]-[4]. The MIMO radar architecture is of two types. One with both the transmitting and receiving antennas or at least one them widely spaced is usually called statistical MIMO radar. Widely spaced antennas enable MIMO systems to view the target from several different angles simultaneously, thereby reducing signal fading caused by RCS fluctuations [1] The other architecture, called collocated MIMO has both the transmitting and receiving antennas closely spaced for detection and direction finding purposes [2], [4]. The Bistatic MIMO radar scheme comes under this category, but with the transmitter and receiver array far apart. Angle estimation in MIMO radar has been researched intensely in recent [9], [10]. In most studies, high resolution subspace based angle estimation algorithms are used based on a circular signal model.

This work was supported by the National Natural Science Foundation of China under Grant No. 61171182.

David Ebregbe and Deng Weibo are with the school of Electronics and Information Engineering, Harbin Institute of Technology, Heilonjiang 150001, Harbin China (e-mail: debregbe@yahoo.co.uk).

Modern telecommunication, satellite and radar systems often use noncircular incoming signals like Binary phase shift keying (BPSK) and M-ary amplitude shift keying (MASK) signals. Circular signals, have Probability density functions (Pdfs) that are circular symmetric. That is, the signal $z(t)$ and its rotation $e^{j\varphi}z$ are equal for any angle, φ. This rotational invariance means the second order statistics only depends on the positive definite hermitian covariance $E\{zz^{H}\}$ because the complementary covariance $E\{zz^{T}\}$ vanishes [16]. On the other hand, signals with noncircular probability density functions (pdfs) retain their complementary covariance as well as their hermitian covariance. This means the second order statistics are also present in the complementary covariance matrix. This non circularity property can be exploited by concatenating the positive definite hermitian covariance and the complementary covariance for aperture extension in radar systems. This increases the angle estimation resolution and also the increases the number of sources that can be detected.

With recent advancements in waveform generation and signal processing technology, waveforms based on Binary phase coded sequences (BPSK) which are noncircular signals, are used in radar, but their noncircularity property is not exploited for angle estimation purpose. They are only used for pulse compression to increase range resolution. In radio communication, the noncircularity of BPSK signals is exploited for bandwidth expansion to transmit information to multiuser environments [12]. Other contributions devoted to exploiting non circularity of noncircular signals include references [5], [6], [13], [16]-[17]. In a similar study, F. Gao et al. [18] show that using the augmented statistics can accommodate the generality of complex signals and also exhibit enhanced performance for situations where the signals are a combination of noncircular and circular signals.

In this paper, we propose a new method that exploits the noncircularity property of non circular signals and the Unitary ESPRIT technique [5], [7], [8] for automatically paired angle estimates for a bistatic MIMO radar system. The rest of the paper is organized as follows: The Non circular signal model for a bistatic MIMO radar system is formulated in Section II; in Section III, we present the unitary transformations of the complex array manifold to a real manifold. The selection matrices for the bistatic MIMO virtual array manifold are also generated; Angle estimation based on Unitary ESPRIT technique is presented in Section IV. Numerical examples are presented and discussed in Section V; and finally we present some conclusions in Section VI.

Notation: $(\cdot)^{H}$, $(\cdot)^{T}$, $(\cdot)^{*}$, $(\cdot)^{-1}$ denote Hemitian transpose, transpose, complex conjugation without transposition and

inverse respectively. diag(·) denotes the diagonalization operation. Vec(·) denotes a matrix operation that stacks the columns of a matrix under each other to form a new vector, **A**(*m,n*) represents the elements of a (*M*×*N*) matrix **A.** ⊗ denotes the kronecker product.

## II. Non Circular Signal Model

Consider a narrowband bistatic MIMO radar system consisting of *M* and *N* half-wavelength spaced omnidirectional antennas for the transmitting and receiving arrays respectively. We assume both arrays are uniform linear arrays (ULA). For simplicity and clarity, we use a simple model with *P* uncorrelated targets with slowly varying velocities in the same range bin. The targets appear in the far field of the transmitting and receiving arrays and have Radar Cross Sections (RCSs) that are constant during a pulse period but fluctuates from pulse to pulse. The target model is a classical Swerling case II model. The directions of the $p^{th}$ target with respect to the transmit array normal and receive array normal are denoted by $\theta_p$ (DOD) and $\phi_p$ (DOA) respectively. The location of the $p^{th}$ target is denoted by ($\theta_p$, $\phi_p$). The transmitted waveforms are *M* orthogonal BPSK modulated signals with identical bandwidth and centre frequency. The transmitted signal of the $m^{th}$ transmit antenna within one repetition interval is denoted by $\mathbf{s}_{mb} = \mathrm{Re}\left\{\mathbf{s}_m e^{j2\pi f_o t}\right\}$, where, $\mathbf{s}_m = e^{j\phi_l} = \pm 1$, $\phi_l = 0$ or $\pi$ radians, are the independent and identically distributed (iid) random BPSK transmitted symbols, $l = 1 \cdots\cdots L$ and *L* denotes the length of the coding sequence within one repetition interval. $\mathbf{s}_{mb}$ is a constant modulus signal i.e. $\left|\mathbf{s}_{mb}(t)\right| = 1$. For a radar system that uses *K* periodic pulse trains to temporally sample the signal environment, the received signals of the $k^{th}$ pulse at the receiver array through reflections of the *P* targets can be written as [9]-[11],

$$\mathbf{X}_k = \sum_{p=1}^{P} \mathbf{a}_r(\phi_p)\beta_p \mathbf{a}_t^T(\theta_p) \begin{bmatrix} \mathbf{s}_{1b} \\ \vdots \\ \mathbf{s}_{Mb} \end{bmatrix} e^{j2\pi f_{dp} t_k} + \mathbf{W}_k \quad (1)$$

where, $\beta_p$ in this case is a real valued amplitude mainly influenced by the reflection gain of the $p^{th}$ target , $f_{dp}$ denotes the Doppler frequency of the $p^{th}$ target, $\boldsymbol{a}_r(\phi_p) = \left[1, e^{jr_p}, e^{j2r_p} \ldots\ldots e^{j(N-1)r_p}\right]^T$ $\sigma^2\mathbf{I}_N$. $\mathbf{I}_N$ is an *N* x *N* identity matrix. $t_k$ denotes the slow time, *k* the slow time index and *K* the number of pulses or repetition intervals. Using the orthogonality property of the transmitted waveforms, the output of the matched filters with the $m^{th}$ transmitted baseband signal can be expressed as

$$\mathbf{Y}_m(t_k) = \sum_{p=1}^{P} \mathbf{a}_r(\phi_p)\beta_p \mathbf{a}_t^T(\theta_p)\mathbf{r}(t_k) \begin{bmatrix} 0 \\ \vdots \\ 1 \\ \vdots \\ 0 \end{bmatrix} e^{j2\pi f_{dp} t_k} + \mathbf{V}_m(t_k) \quad (2)$$

where, $r(t_k) = \mathbf{s}_m e^{j\varphi_p}$, $\varphi_p$ denotes the arbitrary phase of the $p^{th}$ signal assumed to be an independent random variable uniformly distributed between 0 and 2π. $e^{j\varphi p} \neq e^{j\varphi q}$ for any $p \neq q$. $\mathbf{s}_m = \mathbf{s}_m^*$. The data matrix in (2) is usually vectorized by stacking the columns of $\mathbf{Y}_m(t_k)$. Let $\mathbf{z}(t_k) \in C^{MN\times 1}$ be the output of all the received signal.

$$\mathbf{z}(t_k) = \left[\mathbf{Y}_1^T(t_k), \ldots\ldots\ldots, \mathbf{Y}_M^T(t_k)\right]^T \quad (3)$$

$$\mathbf{z}(t_k) = \mathbf{A}\mathbf{u}(t_k) + \mathbf{n}(t_k) \quad (4)$$

where $\mathbf{A} = \left[\mathbf{a}_r(\phi_1) \otimes \mathbf{a}_t(\theta_1), \ldots\ldots\ldots\ldots, \mathbf{a}_r(\phi_p) \otimes \mathbf{a}_t(\theta_p)\right]$ is the $MN \times P$ steering matrix. $\mathbf{n}(t_k) = \mathrm{vec}(\mathbf{V}_m(t_k))$ is the additive white Gaussian noise of zero mean and covariance, $\sigma^2\mathbf{I}_{MN}$ after match filtering. $\mathbf{u}(t_k) = \mathbf{r}(t_k) \begin{bmatrix} \beta_1 e^{j2\pi f_{d1} t_k} \\ \vdots \\ \beta_P e^{j2\pi f_{dP} t_k} \end{bmatrix}$.

Let **Z** denote the $MN \times K$ complex data matrix composed of *K* snapshots of $\mathbf{z}(t_k)$, $1 \le k \le K$.

$$\mathbf{Z} = [\mathbf{z}(t_1)\ \mathbf{z}(t_2) \cdots\cdots \mathbf{z}(t_K)] \quad (5)$$

$$= \mathbf{A}[\mathbf{u}(t_1)\,\mathbf{u}(t_2) \cdots\cdots \mathbf{u}(t_K)] + [\mathbf{n}(t_1)\,\mathbf{n}(t_2) \cdots\cdots \mathbf{n}(t_k)] \quad (6)$$

$$\mathbf{Z} = \mathbf{A}\mathbf{U} + \mathbf{N} \quad (7)$$

$$\mathbf{Z} = \mathbf{A}\boldsymbol{\Delta}\mathbf{S}_p + \mathbf{N} \quad \in C^{MN\times K} \quad (8)$$

where $\boldsymbol{\Delta} = diag(e^{j\varphi_1}, \ldots\ldots\ldots, e^{j\varphi_P})$ and

$\mathbf{S}_p = \mathbf{s}_m[\beta_1 e^{j2\pi f_{d1} t_k} \ldots\ldots \beta_p e^{j2\pi f_{dp} t_k}]^T$, $\mathbf{U} = \boldsymbol{\Delta}\mathbf{S}_p$

To exploit this rotational invariance between the transmitted BPSK symbols and the reflected signals, we concatenate the array measurements **Z** and their conjugate components $\mathbf{Z}^*$ to form the augmented signal model,

$$\mathbf{Z}_{nc} = \begin{bmatrix} \mathbf{Z} \\ \prod_{MN} \mathbf{Z}^* \end{bmatrix} \quad (9)$$

$\prod_{MN}$ is the $MN \times MN$ exchange matrix with ones on its antidiagonal and zeros elsewhere.

$$\begin{aligned}\mathbf{Z}_{nc} &= \begin{bmatrix} \mathbf{A}\,\mathbf{U} \\ \prod_{MN}\mathbf{A}^{*}\boldsymbol{\Delta}^{*}\mathbf{U} \end{bmatrix} + \begin{bmatrix} \mathbf{N} \\ \prod_{MN}\mathbf{N}^{*} \end{bmatrix} \\ &= \begin{bmatrix} \mathbf{A} \\ \prod_{MN}\mathbf{A}^{*}\boldsymbol{\Delta}^{*}\boldsymbol{\Delta}^{*} \end{bmatrix}\mathbf{U} + \begin{bmatrix} \mathbf{N} \\ \prod_{MN}\mathbf{N}^{*} \end{bmatrix}\end{aligned} \tag{10}$$

$$\mathbf{Z}_{nc} = \mathbf{A}_{nc}\mathbf{U} + \mathbf{N}_{nc} \tag{11}$$

## III. Virtual Array Manifold Selection Matrices

We employ the linear algebra property that the inner product between any two conjugate centrosymmetric vectors is real valued. Any matrix whose rows are each conjugate centro symmetric can be applied to transform a complex valued array manifold vector into a real valued manifold. i.e. If the matrix $\mathbf{A}$ is centro hermitian, then $\mathbf{Q}_F^H\mathbf{A}\mathbf{Q}_S$ is a real matrix. The matrix $\mathbf{Q}$ is unitary; its columns are conjugated symmetric and has a sparse structure [15]. As researched by various authors based on the pioneering work of Lee [14], the perfect matrices to accomplish this are

$$\mathbf{Q}_{2F} = \frac{1}{2}\begin{bmatrix} \mathbf{I}_F & j\mathbf{I}_F \\ \prod_F & -j\prod_F \end{bmatrix} \quad \text{for even } F$$

and (12)

$$\mathbf{Q}_{2F+1} = \frac{1}{2}\begin{bmatrix} \mathbf{I}_F & \mathbf{0} & j\mathbf{I}_F \\ \mathbf{0}^T & \sqrt{2} & \mathbf{0}^T \\ \prod_F & \mathbf{0} & -j\prod_F \end{bmatrix} \quad \text{for odd } F$$

These can be used to transform the complex valued data matrix to a real valued matrix.

$$\mathbf{Z}_{real} = \mathbf{Q}_{MN}^H\,\mathbf{Z}_{nc}\,\mathbf{Q}_{2K} \tag{13}$$

The real valued covariance matrix can be estimated using the maximum likelihood estimate,

$$\mathbf{R}_{Z_{real}} = \frac{1}{2K}\left(\mathbf{Z}_{real}\mathbf{Z}_{real}^H\right) \tag{14}$$

Eigen-decomposition of $\mathbf{R}_{Z_{real}}$ yields a signal subspace matrix $\mathbf{E}_S$ composed of the $P$ eigenvectors corresponding to the $P$ largest eigenvalues. Exploiting the double vandermonde in the kronecker product structure of $\mathbf{A}(\theta, \phi)$, similar to the 2D DOA estimation using a URA [8], we have the following selection matrices for the transmit array.

$$\mathbf{J}_{nc1} = \mathbf{I}_{N\times N} \otimes \mathbf{I}_{2\times 2} \otimes \left[\mathbf{I}_{(M-1)\times(M-1)} \quad \mathbf{0}_{(M-1)\times 1}\right] \tag{15}$$

$$\mathbf{J}_{nc2} = \mathbf{I}_{N\times N} \otimes \mathbf{I}_{2\times 2} \otimes \left[\mathbf{0}_{(M-1)\times 1} \quad \mathbf{I}_{(M-1)\times(M-1)}\right] \tag{16}$$

$$\mathbf{J}_{nc2} = \prod_{(M-1)N}\mathbf{J}_{nc1}\prod_{MN} \tag{17}$$

The shift invariance property for the transmit array from the columns of $\boldsymbol{A}$ can be expressed as

$$\mathbf{J}_{nc1}\mathbf{A} = \mathbf{J}_{nc2}\mathbf{A}\boldsymbol{\Phi}_t \tag{18}$$

where, $\boldsymbol{\Phi}_t = diag\left\{e^{jt_p}\right\}_{p=1}^{P}$. The selection matrices for the receive array can also be expressed as

$$\mathbf{J}_{nc3} = \mathbf{I}_{2\times 2} \otimes \left[\mathbf{I}_{M(N-1)\times M(N-1)} \quad \mathbf{0}_{M(N-1)\times M}\right] \tag{19}$$

$$\mathbf{J}_{nc4} = \mathbf{I}_{2\times 2} \otimes \left[\mathbf{0}_{M(N-1)\times M} \quad \mathbf{I}_{M(N-1)\times M(N-1)}\right] \tag{20}$$

and they also posses centrosymmetry with respect to each other.

$$\mathbf{J}_{nc4} = \prod_{M(N=1)}\mathbf{J}_{nc3}\prod_{MN} \tag{21}$$

$$\mathbf{J}_{nc3}\mathbf{A} = \mathbf{J}_{nc4}\mathbf{A}\boldsymbol{\Phi}_r \tag{22}$$

where $\boldsymbol{\Phi}_r = diag\left\{e^{jr_p}\right\}_{p=1}^{P}$.

## IV. Joint Angle Estimation Using Unitary Esprit

The Unitary transformed virtual array steering matrix is obtained as [7], [8]:

$$\mathbf{G} = \mathbf{Q}_{MN}^H\mathbf{A} \tag{23}$$

The transformed selection matrices and invariance equations can be obtained by substituting (27) into (22) and (26).

$$\mathbf{J}_{nc1}\mathbf{Q}_{MN}\mathbf{Q}_{MN}^H\mathbf{A} = \boldsymbol{\Phi}_t\mathbf{J}_{nc2}\mathbf{Q}_{MN}\mathbf{Q}_{MN}^H\mathbf{A} \tag{24}$$

$$\mathbf{J}_{nc1}\mathbf{Q}_{MN}\boldsymbol{G} = \boldsymbol{\Phi}_t\mathbf{J}_{nc2}\mathbf{Q}_{MN}\mathbf{G} \tag{25}$$

Premultiplying both sides by $\boldsymbol{Q}_{(M-1)N}^H$ gives the invariance equation for the transmit array as

$$\mathbf{Q}_{(M-1)N}^H\mathbf{J}_{nc1}\mathbf{Q}_{MN}\mathbf{G} = \boldsymbol{\Phi}_t\mathbf{Q}_{(M-1)N}^H\mathbf{J}_{nc2}\mathbf{Q}_{MN}\mathbf{G} \tag{26}$$

Using (21), $\prod_n\mathbf{Q}_n = \mathbf{Q}_n^*$ and $\prod_n\prod_n = \mathbf{I}_n$

$$\begin{aligned}\mathbf{Q}_{(M-1)N}^H\mathbf{J}_{nc2}\mathbf{Q}_{MN} &= \mathbf{Q}_{(M-1)N}^H\prod_{(M-1)N}\prod_{(M-1)N}\mathbf{J}_{nc2}\prod_{MN}\prod_{MN}\mathbf{Q}_{MN} \\ &= \mathbf{Q}_{(M-1)N}^T\mathbf{J}_{nc1}\mathbf{Q}_{MN}^* \\ &= (\mathbf{Q}_{(M-1)N}^H\mathbf{J}_{nc1}\mathbf{Q}_{MN})^*\end{aligned} \tag{27}$$

$$\mathbf{K}_1 = 2\,\mathrm{Re}\left\{(\mathbf{Q}^H_{(M-1)N}\mathbf{J}_{nc2}\mathbf{Q}_{MN})\right\} \quad (28)$$

$$\mathbf{K}_2 = 2\,\mathrm{Im}\left\{(\mathbf{Q}^H_{(M-1)N}\mathbf{J}_{nc2}\mathbf{Q}_{MN})\right\} \quad (29)$$

Substituting (31) and (32) in (28), we have

$$\left(\mathbf{Q}^H_{(M-1)N}\mathbf{J}_{nc2}\mathbf{Q}_{MN}\right)^* \mathbf{G} = \mathbf{\Phi}_t\left(\mathbf{Q}^H_{(M-1)N}\mathbf{J}_{nc2}\mathbf{Q}_{MN}\right)\mathbf{G} \quad (30)$$

$$\mathbf{\Phi}_t\left(\mathbf{K}_1 - j\mathbf{K}_2\right)\boldsymbol{G} = \left(\mathbf{K}_1 + j\mathbf{K}_2\right)\mathbf{G} \quad (31)$$

Multiplying both sides by $e^{-jt_p/2}$ gives

$$e^{-jt_p/2}\mathbf{\Phi}_t\left(\mathbf{K}_1 - j\mathbf{K}_2\right)\mathbf{G} = e^{-jt_p/2}\mathbf{I}_P\left(\mathbf{K}_1 + j\mathbf{K}_2\right)\mathbf{G} \quad (32)$$

Note that $\mathbf{\Phi}_t = diag\left\{e^{jt_p}\right\}_{p=1}^{P}$, and rearranging we have

$$\left(e^{jt_p/2}\mathbf{I}_P - e^{-jt_p/2}\mathbf{I}_P\right)\mathbf{K}_1\mathbf{G} = j\left(e^{jt_p/2}\mathbf{I}_P - e^{-jt_p/2}\mathbf{I}_P\right)\mathbf{K}_2\mathbf{G} \quad (33)$$

Using the tangent identity

$$\tan\left(t/2\right) = \frac{e^{j\,t/2} - e^{-j\,t/2}}{j\left(e^{j\,t/2} + e^{-j\,t/2}\right)} \quad (34)$$

$$diag\left\{\tan\left(t_p/2\right)\right\}_{p=1}^{P}\mathbf{K}_1\mathbf{G} = \mathbf{K}_2\mathbf{G} \quad (35)$$

We obtain the following transformed real valued invariance equation for the transmit array.

$$\mathbf{K}_1\mathbf{G}\mathbf{\Omega}_t = \mathbf{K}_2\mathbf{G} \quad (36)$$

where $\mathbf{\Omega}_t = diag\left\{\tan\left(t_p/2\right)\right\}_{p=1}^{P}$

The $2MN \times P$ real valued matrix of signal eigenvectors $\mathbf{E}_s$ spans the same $P$ dimensional subspace as the $2MN \times P$ real valued steering matrix $\mathbf{G}$. Therefore there exists a nonsingular matrix $\mathbf{H}$ of size $P \times P$ such that $\mathbf{E}_s = \mathbf{GH}$. Substituting this in (40) yields the transformed invariance equation from which we can compute the DODs.

$$\mathbf{K}_1\mathbf{E}_s\mathbf{\Psi}_t = \mathbf{K}_2\mathbf{E}_s \quad (37)$$

where $\mathbf{\Psi}_t = \mathbf{H}\mathbf{\Omega}_t\mathbf{H}^{-1}$. Following the same procedure, the transformed selection matrices and invariance equations to compute the DOAs for the receiver array are obtained as

$$\mathbf{K}_3 = 2\,\mathrm{Re}\left\{(\mathbf{Q}^H_{M(N-1)}\mathbf{J}_{nc4}\mathbf{Q}_{MN})\right\} \quad (38)$$

$$\mathbf{K}_4 = 2\,\mathrm{Im}\left\{(\mathbf{Q}^H_{M(N-1)}\mathbf{J}_{nc4}\mathbf{Q}_{MN})\right\} \quad (39)$$

$$\mathbf{K}_3\mathbf{G}\mathbf{\Omega}_r = \mathbf{K}_4\mathbf{G} \quad (40)$$

where $\mathbf{\Omega}_r = diag\left\{\tan\left(r_p/2\right)\right\}_{p=1}^{P}$. And the invariance equation from which to compute the DOAs is obtained as

$$\mathbf{K}_3\mathbf{E}_s\mathbf{\Psi}_r = \mathbf{K}_4\mathbf{E}_s \quad (41)$$

where $\mathbf{\Psi}_r = \mathbf{H}\mathbf{\Omega}_r\mathbf{H}^{-1}$.

Since both $\mathbf{\Psi}_t$ and $\mathbf{\Psi}_r$ share the same transform matrix $\boldsymbol{H}$ and are also real valued matrices, automatically paired estimates of DODs and DOAs $\left\{u_p, r_p\right\}, p = 1 \cdots\cdots P$ can be obtained from the real and imaginary parts of the eigenvalues obtained by the eigendecomposition of the complex valued matrix

$$\mathbf{\Psi}_t + j\mathbf{\Psi}_r = \mathbf{H}\left(\mathbf{\Omega}_t + j\mathbf{\Omega}_r\right)\mathbf{H}^{-1} \quad (42)$$

where $\mathbf{\Omega}_t + j\mathbf{\Omega}_r = diag\left\{\lambda_p\right\}_{p=1}^{P}$, are the eigenvalues. The DODs and DOAs are obtained as

$$\hat{\theta}_p = \arcsin\left\{2\arctan\left(\mathrm{Re}\left\{\lambda_p\right\}\right)\right\} \quad 1 \le p \le P \quad (43)$$

$$\hat{\phi}_p = \arcsin\left\{2\arctan\left(\mathrm{Im}\left\{\lambda_p\right\}\right)\right\} \quad 1 \le p \le P \quad (44)$$

## V. Simulation Results

In this section, we present some numerical examples, using monte Carlo simulations to demonstrate the effectiveness of the method proposed in this paper.

First, we consider a uniform linear array (ULA) of 3 antennas at the transmitter and 4 antennas at the receiver, both of which have half wavelength spacing between its antennas. There are 6 independent BPSK signals impinging on the virtual array from 6 different targets with angles and initial phases as shown in Table I and a signal-to-noise ratio SNR=10dB.

TABLE I
Target Signal Parameters

| Targets | 1 | 2 | 3 | 4 | 5 | 6 |
|---|---|---|---|---|---|---|
| DOD(θ) | $0^0$ | $10^0$ | $30^0$ | $60^0$ | $20^0$ | $50^0$ |
| DOA(ϕ) | $-10^0$ | $20^0$ | $25^0$ | $20^0$ | $50^0$ | $60^0$ |
| Phases | π/2 | π/4 | π/6 | π/8 | π/5 | π/3 |

We observed 256 snapshots of the received signal corrupted by a zero mean spatially white noise of variance = 1. For

purpose of statistical repeatability, we made 500 monte carlo trials. Fig. 1 shows the targets are well localized and correctly paired.

In the second part of the simulation, we demonstrate the performance improvement due to non circularity property. This gives an indication of the information contributed by the complementary covariance matrix. We use the Root Mean Square Error (RMSE) performance criterion. The RMSE of the $p^{th}$ target angle estimation is defined as

$$\text{RMSE}_p = \sqrt{1/L \sum_{l=1}^{L} \left(\hat{\theta}_{pl} - \theta_p\right)^2 + \left(\hat{\phi}_{pl} - \phi_p\right)^2}$$

where, $L$ is the monte carlo trial number, $\hat{\theta}_{pl}$ and $\hat{\phi}_{pl}$ are the estimates at the $l^{th}$ iteration, $\theta_p$ and $\phi_p$ are true angle values. We compare the RMSE of target angle estimation of the proposed algorithm to that of the same non circular signal but using only the standard hermitian covariance matrix. Considering the same number and configuration of antennas as before, we vary the signal to noise ratio (SNR) from -5 to 30dB. Results were obtained using 200 monte carlo simulations. Fig. 2 shows the RMSE versus SNR for the 6 targets. The estimation errors are quite negligible. Fig. 3 shows a comparison of the RMSE of angle estimation for our proposed algorithm and the RMSE of angle estimation using the same BPSK signal without exploiting the conjugate symmetry. It can be seen from Fig. 3, that that for as low as -5dB SNR, the proposed algorithm yields excellent estimates with negligible errors. Furthermore, this algorithm which uses both the hermitian covariance and the complementary covariance clearly outperforms the circular model Unitary ESPRIT algorithm that uses only the hermitian covariance. Performance improvement is observed for both low and high SNRs.

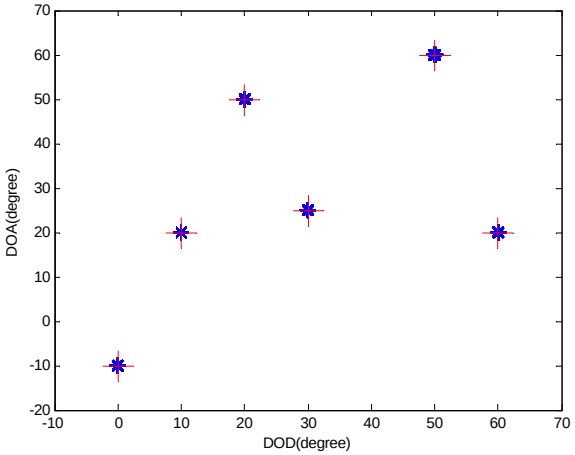


Fig. 1 Joint angle estimation of the proposed algorithm for 6 targets over 500 monte carlo trials with SNR =10dB

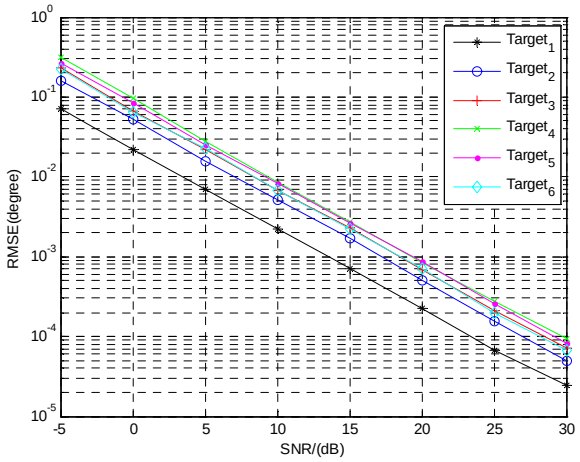


Fig. 2 RMSE of angle estimation for the six targets versus SNR for $K$=256 samples and 200 monte carlo trials

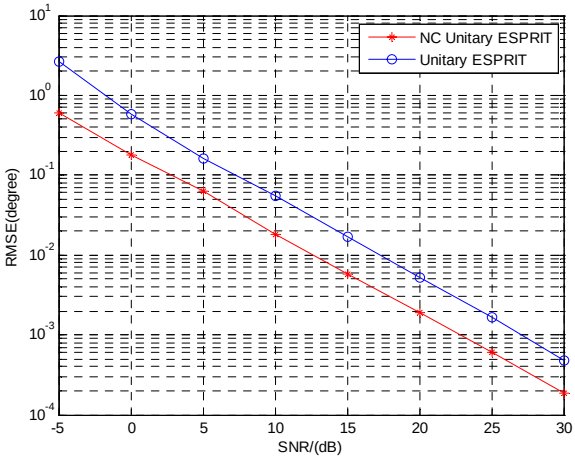


Fig. 3 RMSE of estimation versus SNR for $M$=$N$=3 antennas and $K$=256 samples for 200 monte carlo trials

In the final simulation test, we perform an asymptotic analysis of the performance of the proposed algorithm and the circular model with respect to the number of transmit/receive antennas. Simulation conditions and parameters are the same as the previous simulations. However, in this case, the number of transmit and receive elements are made equal i.e $M = N$ for ease of presentation. Fig. 4 shows the RMSE of angle estimation versus the number of transmit/receive antennas at a SNR of 20dB. As expected asymptotically, both algorithms improve as the number of sensors increase with our proposed noncircular model consistently giving lower angle estimation errors.

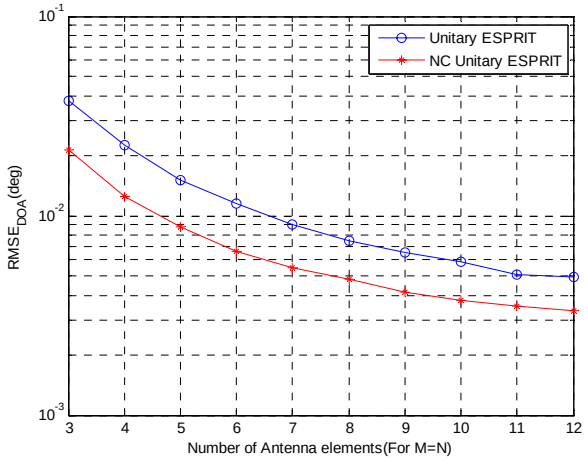


Fig. 4 RMSE of estimation for different values of *M*=*N*, *K*=256 samples and 200 monte carlo trials

## VI. Conclusions

We have investigated the effectiveness of using the second order statistical information contained in both the hermitian covariance matrix and the elliptic covariance matrix of a non circular signal for aperture extension. Exploiting the non circularity property of non circular signals, like BPSK signals as shown in our simulation results, gives a better estimator performance and increases the number of targets that can be detected.

## References

[1] A.M. Haimovich, R. Blum, L. Cimini, "MIMO radar with widely separated antennas", IEEE Signal Processing Magazine 25 (1) (2008) 116–129.

[2] Fisher, E., Haimovich, A., and Blum, R.S., et al.: 'MIMO radar: an idea whose time has come'. Proc. IEEE Radar Conf., Philadelphia, PA, USA, April 2004, pp. 71–78.

[3] J. Li, P. Stoica, "MIMO radar with colocated antennas", IEEE Signal Processing Magazine 24 (5) (2007) 106–114.

[4] I. Bekkerman, J. Tabrikian, "Target detection and localization using MIMO radars and sonars", IEEE Transactions on Signal Processing 54 (10) (2006) 3873–3883.

[5] M. Haardt and F. Roemer, "Enhancements of Unitary ESPRIT for non-circular sources", in *Proc. IEEE International Conference on Acoustics, Speech and Signal Processing (ICASSP 2004)*, vol. 2, pp. 101–104, Montreal, Canada, May 2004.

[6] P. Charg´e, Y. Wang, and J. Saillard, "A non circular sources direction finding method using polynomial rooting", *Signal Processing*, vol. 81, pp. 1765–1770, 2001.

[7] M. Haardt and J. A. Nossek, "Unitary ESPRIT: How to obtain increased estimation accuracy with a reduced computational burden", *IEEE Trans. Signal Processing*, vol. 43, pp. 1232–1242,1995.

[8] Zoltowski, M.D., Haardt, M., and Mathews, C.P.: 'Closed-form 2-D angle estimation with rectangular arrays in element space or beamspace via Unitary ESPRIT', IEEE Trans. Signal Process., 1996, 44, (2), pp. 316-328.

[9] M. Jin, G. Liao and J. Li, "Joint DOD and DOA estimation for bistatic MIMO radar", Elsevier Signal. Processing 89 244-251 2009.

[10] M. L. Bencheikh, Y. Wang and H. He, "Polynomial root finding technique for joint DOA DOD estimation in bistatic MIMO radar", Signal Processing (EURASIP), 2010, 90(9), pp.2723-2730

[11] J.L. Chen, H. Gu, W.M. Su, "A new method for joint DOD and DOA estimation in bistatic MIMO radar", Signal Processing 90 (2010) 714–718.

[12] Barbaresco, F., and Chevalier, P.: 'Noncircularity exploitation in signal processing overview and application to radar'. IET Waveform Diversity and Digital Radar Conf., London, UK, 2008, pp. 1-6.

[13] B. Picinbono, "On circularity", *IEEE Trans. Signal Processing*, Vol 42, No 12, pp. 3473-3482, Dec. 1994.

[14] A. Lee, "Centrohermitian and skew-centrohermitian matrices," *Linear Algebra and its Applications*, vol. 29, pp. 205–210, 1980.

[15] N. Yilmazer, J. Koh, T.K. Sarkar," Utilization of a unitary transform for efficient computation in the matrix pencil method to find the direction of arrival", IEEE Trans. Antennas Propagation. 54 (1) (2006) 175-181.

[16] S. Javidi, D.P. Mandic, C. C. Took and A. Cichocki, "Kurtosis-based blind source extraction of complex non‐circular signals with application in EEG artifact removal in real-time" Frontiers in Neuroscience, Volume 5. Article 105, October 2011.

[17] J. Galy, C. Adnet, "Blind separation of non-circular sources", in: Proceedings of the Tenth IEEE Workshop on Statistical Signal and Array Processing, 2000, pp 315-318.

[18] F. Gao, Y. Wang, A. Nallanathan, "Improved MUSIC by Exploiting Both Real and Complex Sources" in *Proc. IEEE International Conference on Military Communications (MILCOM 2006)* Washington, DC pp 1-6 2006.